

## Partial Volume Correction for $^{23}\text{Na}$ MRI of Human Brain

Sebastian C. Niesporek<sup>1</sup>, Stefan H. Hoffmann<sup>1</sup>, Moritz C. Berger<sup>1</sup>, and Armin M. Nagel<sup>1</sup>

<sup>1</sup>Medical Physics in Radiology, German Cancer Research Center (DKFZ), Heidelberg, Germany

**INTRODUCTION** Sodium ( $^{23}\text{Na}$ ) MRI is applied in a wide range of biomedical research application [1]. However, compared to conventional  $^1\text{H}$  MRI, much larger voxel sizes have to be used due to low MR sensitivity and low *in-vivo* concentrations of the  $^{23}\text{Na}$  nucleus. Additionally,  $^{23}\text{Na}$  exhibits fast  $T_{2^*}$ -relaxation and, thus,  $^{23}\text{Na}$  MRI requires specially adapted pulse sequences such as 3D radial or twisted projection imaging [2]. However, these pulse sequences have larger full widths at half maximums (FWHM) of the *point spread functions* (PSF) compared to Cartesian sampling schemes. The fast  $T_{2^*}$ -relaxation leads to an additional broadening of the PSF. These effects lead to partial volume effects that decrease the accuracy of quantitative  $^{23}\text{Na}$  MRI measurement in particular if small structures ( $\leq 1\text{mm}$ ) are investigated. The partial spread of neighboring structures (spill-in/out) can be corrected by various correction methods, which were originally designed for positron emission tomography applications [3]. In this study we transferred the method of Rousset (known as *geometric transfer method* (GTM)) [4] to  $^{23}\text{Na}$  MRI. The method was optimized with respect to the relevant MRI parameters. Evaluation of the GTM algorithm was done in simulations, phantom studies and in  $^{23}\text{Na}$  MRI of the human brain.

**METHODS** A phantom (Fig.1) was designed to test the performance of the implemented *partial volume correction* (PVC) algorithm for  $^{23}\text{Na}$  MRI. PMMA-tubes with inner diameter ranging from 10-64mm were filled with different sodium concentrations (17-207mmol/L). Imaging was conducted on a 7T MR system (Magnetom 7T, Siemens AG, Healthcare Sector, Erlangen, Germany).  $^{23}\text{Na}$  MRI was performed with a density adapted projection pulse sequence (3D-DAPR) (TR/TE=50ms/0.35ms, 20000 projections,  $\Theta=70^\circ$ , nominal resolution:  $(3\text{mm})^3$  /  $(5\text{mm})^3$ ;  $T_{\text{Acq}}=16:40\text{mins}$ , Fig.1, left) and PVC was performed with structural knowledge drawn from high resolution  $^1\text{H}$  data (Fig.1, right). The same steps were applied to simulated data to verify PVC in the phantom by simulation.

**In-vivo  $^{23}\text{Na}$  MRI:** PVC was applied to a data set of a healthy volunteer to correct the sodium signal in different brain compartments and to determine the sodium concentrations.  $^{23}\text{Na}$  MRI was performed with 3D-DAPR pulse sequence (TR/TE=200ms/0.35ms, 3800 projections,  $(3\text{mm})^3$ ,  $\Theta=90^\circ$ ,  $T_{\text{Acq}}=12:00\text{mins}$ , Fig.3.1). Proton data sets were acquired with a MPRAGE (TR/TE=3400ms/1.99ms,  $\Theta=9^\circ$ ,  $0.6\text{ mm}^3$ ) and a CISS sequence (TR/TE=5.01ms/2.2ms,  $\Theta=16^\circ$ ,  $0.7\text{ mm}^3$ ) which enabled better segmentation due to different  $T_1$  and  $T_2$  contrast. Image registration and segmentation was performed with the FMRIB Software Library (FSL) [5] using a rigid body algorithm with 9 degrees of freedom (FLIRT) [6] and the FMRIB's Automated Segmentation Tool [7]. Normalization of the sodium signal was done by two separate tubes with known concentration (103/155 mmol/L) placed next to the volunteer's head. To check the performance of the experiment, the ventricle and remaining CSF where considered as two individual compartments where one would expect the same sodium concentration ( $c_{\text{CSF}} = 140-145\text{ mmol}$ ) in both compartments.

**RESULTS** The phantom studies showed an overall improvement (8-15%) of the determined concentrations after applied PVC in both, simulation and measurement. The values of all sample concentrations and the PMMA compartment are plotted as a function of input concentration before and after PVC (Fig.2). After PVC the determined concentrations are closer to the expected values (Fig.2, bottom). The improvement for the *in-vivo* signal intensities shows the expected behavior (Tab.1) for all compartments. Gray and White Matter values are corrected up-, CSF values downward. The small structures of the outer CSF compartment (sulci) experience strongest correction (+85%) and the discrepancy between the two CSF compartments is lowered from 42.5% before to 14.4% after correction. Evaluation of a second data set showed the same behavior for all compartments and similar discrepancy for the two CSF volumes. A lower resolution data set was also taken for segmentation (MPRAGE,  $(1\text{mm})^3$ ) what yielded to a higher (19.3%) discrepancy.

**DISCUSSION** Correct choice of the PSF and proper segmentation led to improved accuracy of concentration measurements in simulated and phantom data. The same result was seen in an *in-vivo* experiment, where segmentation on a higher resolution proton data set led to a better recovery of the brain compartment intensities. Non-optimal segmentation and registration can lead to larger errors, thus a good segmentation is crucial. The discrepancy between two individually treated CSF compartments was markedly lowered. Values for white and grey matter are also in the expected range.

**CONCLUSION** The proposed method improves the accuracy of concentration measurements in  $^{23}\text{Na}$  MRI. It can also be transferred to MRI of other x-nuclei with short relaxation times and low SNR (e.g.  $^{17}\text{O}$ ,  $^{35}\text{Cl}$ ,  $^{39}\text{K}$ ).

Compartment	Pre-PVC [mmol/L]	Post-PVC [mmol/L]	Change [%]
CSF	69 $\pm$ 9	131 $\pm$ 9	+85
GM	57 $\pm$ 3	46 $\pm$ 3	-13
WM	45 $\pm$ 3	40 $\pm$ 3	-20
Ventricle	120 $\pm$ 8	153 $\pm$ 8	+26

**Tab.1:** Results of *in-vivo* experiment, determined concentration for different brain compartments

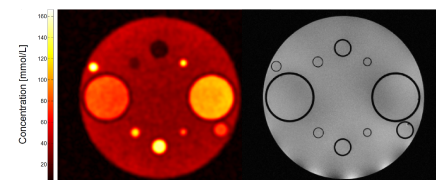


**Fig. 1:** PVC Phantom, sodium image (left), registered  $^1\text{H}$  image (right) ( $(0.65\text{ mm})^3$ , TR=6.9ms, TE=2.99ms)

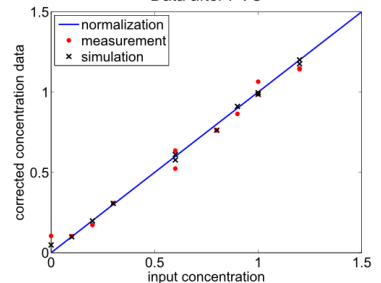
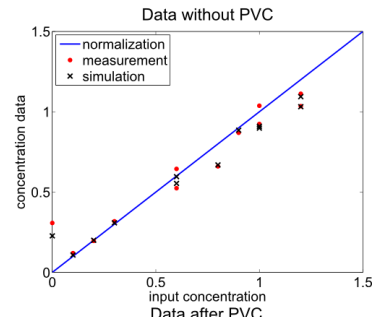


**Fig. 2:** Result before (top) and after (bottom) correction, simulated (black) and measured (red) data

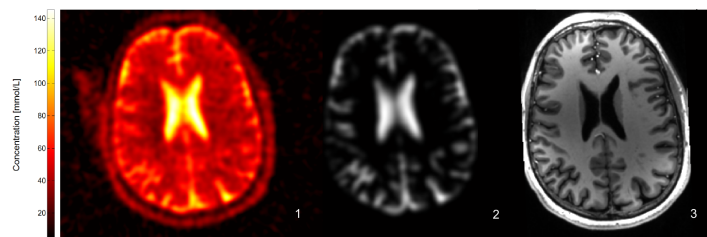


**Fig. 3:** Data used for PVC, sodium image (1), convoluted segmentation (2), co-registered  $^1\text{H}$ -image for segmentation (3)

## REFERENCES

- [1] Madelin, G., Regatte, R. R., *JMRI* 2013 (38) p. 511-29, [2] Konstandin S, Nagel AM., *MAGMA* 201, doi: 10.1007/s10334-013-0394-3, [3] Hoetjes, *Eur J Nucl Med Mol Imaging*, 37:1679–1687, 2010, [4] Rousset, *J Nucl Med*, 5:904-911, 1998, [5] Smith SM, Jenkinson M, Woolrich MW, et al. *NeuroImage*. 2004;23 Suppl 1:S208-19, [6] Jenkinson Met al. , *NeuroImage*. 2002;17(2):825-41, [7] Zhang Y, Brady M, Smith S, *IEEE Trans Med Imag*, 20(1):45-57, 2001